LUMPED PARAMETER MODELLING AND SIMULATION OF A SIMPLIFIED VOCAL APPARATUS IN THE PORT-HAMILTONIAN FRAMEWORK

Thomas Risse, Thomas Hélie, Fabrice Silva, Victor Wetzel

forum acusticum 2023

LUMPED PARAMETER MODELLING AND SIMULATION OF A SIMPLIFIED VOCAL APPARATUS IN THE PORT-HAMILTONIAN FRAMEWORK

Thomas Risse[1*] **Thomas Hélie**[1] **Fabrice Silva**[2]
Victor Wetzel[1]
[1] STMS laboratory (IRCAM-CNRS-SU), Paris, France
[2] Aix Marseille Univ, CNRS, Centrale Marseille, LMA UMR 7031, Marseille, France

ABSTRACT

In this work, we propose a power-balanced model of the full vocal apparatus, described by passive elementary components, the connection of which accounts for fluid-solid and fluid-fluid interactions.

In the larynx, we consider a potential incompressible flow of an inviscid fluid between parallel moving walls whose dynamics is reduced to a mass-spring-damper oscillator equipped with an elastic cover. The vocal tract is represented by a macroscopic lumped parameter model derived for the irrotational flow of a compressible inviscid fluid with the simplest kinematics satisfying the boundary conditions.

The assembly of elements admits a representation as a constrained global port-Hamiltonian system for which we propose simulations based on a projection method that preserves the power balance. Several numerical experiments show the ability of the model to reproduce a variety of regimes according to different configurations: non oscillating regimes (no phonation), periodic regimes (typical of healthy voice) and non-periodic oscillating regimes (typical of dysphonia). These simulations are used to sketch first cartographies of regimes with respect to control parameters.

Keywords: Physical modelling, Vocal apparatus, Port-Hamiltonian Systems, Lumped parameter models

*__Corresponding author__: thomas.risse@ircam.fr.

1. INTRODUCTION

Physical modelling of the vocal apparatus has a long history, based on low or high dimensional descriptions. For the larynx, the first family includes lumped-parameters models such as the reference two-mass model presented in [1]. It accounts for a one-dimensional glottal flow coupled to two pairs of mass-spring-damper systems representing trapezoidal vocal folds, the flow dynamics being governed by a Bernoulli equation. Extensions to refined shapes and structures are also available in e.g. [2–4]. However, such Bernoulli-based modelling does not represent balanced power exchanges between the glottal flow and the vocal folds.

The second family based on e.g. finite element methods and coupled fluid-structure interactions (FSI) solvers is computationally highly demanding (see e.g. [5] and [6] for 2D and 3D problems, or the European project EUNISON).

This work is twofold and aims to: develop a lumped-parameter model of a full vocal apparatus that accounts for balanced power exchanges between the glottal flow and the vocal folds; provide a power-balanced simulation that requires a relatively low computational cost. In order to do so, we use the port-Hamiltonian framework by assembling models from Refs. [7] and [8] (see also [9]).

This paper is organised as follows. Section 2 presents a brief reminder on Port-Hamiltonian systems and detail the modelling of the larynx, the vocal tract and their assembly. Section 3 presents the power-balanced numerical method. and section 4 the numerical experiments, before conclusions and perspectives in section 5.

2. MODELLING

2.1 Reminder on Port Hamiltonian Systems

We propose here a short presentation of port-Hamiltonian systems (PHS), introduced in [10]. The port-Hamiltonian framework is an extension of classical autonomous and conservative Hamiltonian mechanics to the cases where internal dissipation of energy and power exchanges with the environment can occur. Their advantages for the representation of multi-physical problems include a natural fulfilment of the power balance, taking into account power exchanges between passive components, hence leading to globally passive systems. We are also particularly interested in the workflow provided by the framework which consists of modelling subsystems separately and connecting them through their interacting port.

We here use the following class of PHS:

$$\underbrace{\begin{bmatrix} \dot{x} \\ w \\ 0 \\ y \end{bmatrix}}_{f} = S \underbrace{\begin{bmatrix} \nabla H(x) \\ z(w,x) \\ \lambda \\ u \end{bmatrix}}_{e}, \text{ with } S = -S^{\intercal}, \tag{1}$$

where $x \in \mathbb{R}^{N_x}$ is the state of the system, $H : \mathbb{R}^{N_x} \to \mathbb{R}$ is the Hamiltonian (positive definite energy function), $w \in \mathbb{R}^{N_w}$ denotes flow variables associated with instantaneous effort laws $z : \mathbb{R}^{N_x+N_w} \to \mathbb{R}^{N_w}$ satisfying $z(w,x)^{\intercal} w \geq 0$, $\lambda \in \mathbb{R}^{N_\lambda}$ denotes Lagrange multipliers relative to constraints on efforts, $y \in \mathbb{R}^{N_{ext}}$ and $u \in \mathbb{R}^{N_{ext}}$ are respectively the outputs and inputs of the system.

The efforts $e \in \mathcal{E} = \mathbb{R}^N$ and flows $f \in \mathcal{F} = \mathbb{R}^N$ define the bond variables $(e, f) \in \mathcal{B} = \mathcal{E} \times \mathcal{F}$ equipped with the pairing $\langle e|f \rangle_{\mathcal{B}} = e^{\intercal} f \in \mathbb{R}$. Detailing variables in e and f (see (1)), this pairing defines a global power as

$$\langle e|f \rangle_{\mathcal{B}} = \underbrace{\nabla H(x)^{\intercal} \dot{x}}_{\text{Stored power}} + \underbrace{z(w,x)^{\intercal} w}_{\text{Dissipated power}} + \underbrace{u^{\intercal} y}_{\text{Exchanged power}}. \tag{2}$$

Note that constraints do not produce work as their power is $\lambda^{\intercal} 0 = 0$ in the pairing.

The skew-symmetry of the interconnection matrix S that links e and f in (1) and characterize the structure of the physical system guarantees the power balance, since $\langle e|f \rangle_{\mathcal{B}} = \langle e|Se \rangle_{\mathcal{B}} = e^{\intercal} S e = 0$.

This matrix is associated with the so-called Dirac structure which gathers compatible efforts and flows:

$$\mathcal{S} = \{(f, e) \in \mathcal{F}, \mathcal{E} | f = Se\}. \tag{3}$$

For our models, this matrix will have the following structure:

$$S = \left[\begin{array}{c|c|c|c} S_{xx} & S_{xw} & S_{x\lambda} & S_{xu} \\ \hline -S_{xw}^{\intercal} & 0 & 0 & S_{wu} \\ \hline -S_{x\lambda}^{\intercal} & 0 & 0 & S_{\lambda u} \\ -S_{xu}^{\intercal} & -S_{wu}^{\intercal} & -S_{\lambda u}^{\intercal} & 0 \end{array}\right]. \tag{4}$$

The next sections are devoted to the description of the two components of our model of the vocal apparatus.

2.2 Larynx

For the larynx, we use a simplified model presented in [7]. It considers a potential incompressible flow of an inviscid fluid between parallel moving walls. Those correspond to the surface of the vocal folds whose dynamics is reduced to a mass-spring-damper oscillator equipped with an elastic cover.

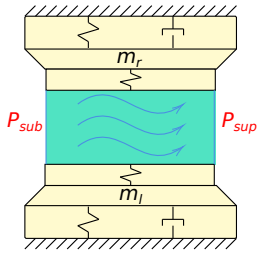

Figure 1. Larynx model schematic.

2.2.1 *Glottal flow*

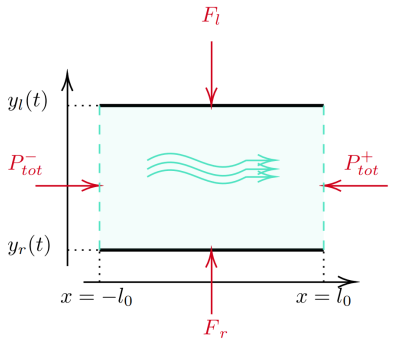

Figure 2. Glottal flow schematic, from [7].

The domain containing the fluid is represented in Fig. 2. Denoting $h = y_l - y_r$ the height of the canal

and $y_m = (y_r + y_l)/2$ the middle-line position, the simplest kinematics for the fluid in the domain obeying Euler equations and satisfying normal velocity continuity on the walls is given by

$$v = \begin{bmatrix} v_x \\ v_y \end{bmatrix} = \begin{bmatrix} v_0 - x\frac{\dot{h}}{h} \\ \dot{y}_m + \frac{\dot{h}}{h}(y - y_m) \end{bmatrix}. \tag{5}$$

In [7], the state vector is $x^{g_0} = \left[v_0, \dot{y}_m, \dot{h}, h\right]$ where v_0 and $\dot{y}_m$ are the mean axial and transverse velocities, h the height of the domain and $\dot{h}$ its time derivative. The Hamiltonian is then given by

$$\frac{1}{2}\left(m(h)v_0^2 + m(h)\dot{y}_m^2 + m_3(h)\dot{h}^2\right), \tag{6}$$

where we consider $m(h) = 2\rho l_0 L h(t)$ the mass of the fluid and $m_3(h) = m(h)(1 + 4l_0^2/h^2)/12$ the effective mass for the transverse expansion motion. However, this choice leads to a state-dependant interconnection matrix, which complicates the implementation of the numerical solver. In order to obtain a PHS representation with a constant interconnection matrix, we here use a change of variable. After introducing a normalisation height h_0, we define $\pi_x = mv_0h_0/h$ and $\pi_y = mv_yh_0/h$ the mean axial and transverse momenta and $\pi_{exp} = 2m_3\dot{h}$ the expansion motion momentum from which we can define the new state vector

$$x^g = [\pi_x, \pi_y, \pi_{exp}, \dot{h}]. \tag{7}$$

The corresponding Hamiltonian is

$$H(x^g) = \frac{h^2}{2h_0^2}\frac{\pi_x^2 + \pi_y^2}{m(h)} + \frac{1}{8}\frac{\pi_{exp}^2}{m_3(h)}. \tag{8}$$

Using this new set of variable and a couple of instantaneous laws modulating the input forces by h_0/h, we obtain the following PHS with a constant interconnection matrix:

$$\left[\begin{array}{c} \dot{\pi_x} \\ \dot{\pi_y} \\ \dot{\pi_{exp}} \\ \dot{h} \\ \hline w_{\text{turb}} \equiv Q^+ \\ w_{g0} \equiv F_l - F_r \\ w_{g1} \equiv \nabla_{\pi_y} H(x) \\ \hline -Q^- \\ Q^+ \\ -v_l \\ -v_r \end{array}\right] = S^{\text{glottal}} \left[\begin{array}{c} \nabla_{\pi_x} H(x) \\ \nabla_{\pi_y} H(x) \\ \nabla_{\pi_{exp}} H(x) \\ \nabla_h H(x) \\ \hline z_{\text{turb}}(w_{\text{turb}}, h) \\ z_{g0}(w_{g1}, h) \\ z_{g1}(w_{g0}, h) \\ \hline P_{tot}^- \\ P^+ \\ F_l \\ F_r \end{array}\right]. \tag{9}$$

This PHS is controlled by subglottal (upstream) and supglottal (downstream, after turbulence dissipation z_{turb}) pressures P_{tot}^- and P^+ and by the forces applied by the left and right vocal folds on the fluid F_l and F_r. The power conjugated outputs are the volume flows $-Q^-$, Q^+ and the speeds $-v_l$ and $-v_r$ of the vocal fold walls.

The dissipation function

$$z_{\text{turb}}(w_{\text{turb}}, h) = \frac{\rho}{2}\left(\frac{w_{\text{turb}}}{L_0 h_0}\right)^2 \Theta(w_{\text{turb}}), \tag{10}$$

with Θ the Heaviside function, represents the loss of energy due to shear layer vortices at the output of the glottis where a rapid change of section is observed.

The instantaneous law

$$\begin{bmatrix} z_{g0} \\ z_{g1} \end{bmatrix} = \frac{h_0}{h}\begin{bmatrix} w_{g1} \\ -w_{g0} \end{bmatrix}, \tag{11}$$

corresponds to a gyrator modulating the forces F_l and F_r in order to keep S^{glottal} constant, without contribution to the power balance as $\langle z_g(w_g, h)|w_g\rangle = 0$.

Finally, the constitutive block matrices of $S^{glottal}$, encoding the dynamics, are

$$S_{xx}^{glottal} = \begin{bmatrix} 0 & 0 & 0 & 0 \\ 0 & 0 & 0 & 0 \\ 0 & 0 & 0 & -2 \\ 0 & 0 & 2 & 0 \end{bmatrix}, \tag{12a}$$

$$S_{xw}^{glottal} = \begin{bmatrix} -L_0h_0 & 0 & 0 \\ 0 & 0 & 1 \\ 2L_0l_0 & 0 & 0 \\ 0 & 0 & 0 \end{bmatrix}, \tag{12b}$$

$$S_{xu}^{glottal} = \begin{bmatrix} L_0h_0 & 0 & -L_0h_0 & 0 \\ 0 & 0 & 0 & 0 \\ 2L_0l_0 & 2L_0l_0 & -1 & -1 \\ 0 & 0 & 0 & 0 \end{bmatrix}, \tag{12c}$$

$$S_{wu}^{glottal} = \begin{bmatrix} 0 & 0 & 0 & 0 \\ 0 & 0 & 1 & -1 \\ 0 & 0 & 0 & 0 \end{bmatrix}. \tag{12d}$$

2.2.2 *Vocal folds*

Vocal folds are reduced to mass-spring-damper systems with a purely elastic cover, as shown in figure 1. The PHS corresponding to this system is presented in [7] and not reproduced here for the sake of brevity.

2.2.3 *Complete larynx*

Once the models of glottal flow and vocal folds are established, they can be connected by means of a PHS connections procedure, as presented in [11]: the output forces of the vocal folds models are linked to the input forces F_l and F_r applied on the glottal flow. The complete larynx model then admits two input-output pairs:

$$u^{larynx} = \left[P_{tot}^{-}, P^{+}\right]^{\intercal} \text{ and } y^{larynx} = \left[-Q^{-}, Q^{+}\right]^{\intercal}, \tag{13}$$

which are respectively the pressures and volume flows at the entrance and exit of the glottis.

2.3 Vocal tract

We use the vocal tract model developed in [8, chap. 3]. It is a lumped parameter model based on the decomposition of the complete vocal tract in multiple sub-tracts. The full tract is then controllable by means of input and output fluid enthalpy and of the velocity of the surrounding tissues. This allows the reproduction of articulations from geometric trajectories to produce vowel sounds.

2.3.1 *A single sub-tract*

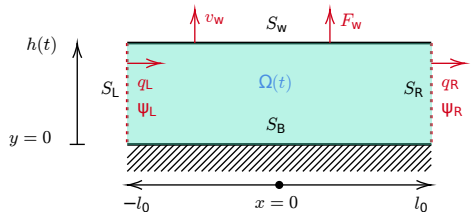

Figure 3. Single tract schematic

We consider a time-varying fluid domain, as presented figure 3. After making the assumption that the fluid is a compressible perfect gas having an homogeneous density in the domain $\Omega(t)$ and that the flow is irrotational, one can derive a finite-dimensional representation of the dynamics, based on a decomposition of the velocity field in 3 different components:

$$v(x,y,t) = \underbrace{\begin{bmatrix}1\\0\end{bmatrix} v_{mx}(t)}_{\text{Uniform axial}} + \underbrace{\begin{bmatrix}-x/h(t)\\ y/h(t)\end{bmatrix} v_y(t)}_{\text{Incompressible}} + \underbrace{\begin{bmatrix}x/l_0\\0\end{bmatrix} v_c(t)}_{\text{Compressibility}}. \tag{14}$$

After some computations presented in [8], Wetzel showed that the dynamics of this single tract admits a port-Hamiltonian formulation with canonical interconnection matrix S (composed of 0, 1 and -1). The state vector for this PHS is given by

$$x^{tract} = [\nu_l, \nu_r, \pi_y, m, h]^{\intercal}, \tag{15}$$

where ν_l and ν_r are axial kinematics variables and π_y is an incompressible transverse motion component. Finally, m and h are respectively the mass of the fluid contained in the tract and the height of the tract. The Hamiltonian associated with these states is given by

$$\begin{aligned} H^{tract}(x^{tract}) = \frac{m}{2l_0^2}(\nu_l^2 + \nu_r^2 - \nu_l\nu_r) + \frac{3\pi_y^2}{2m} \\ + P_0 h S_w \left[\frac{\gamma}{2}\left(\frac{\rho(m,h)-\rho_0}{\rho_0}\right) - 1\right], \end{aligned} \tag{16}$$

where $\rho(m,h) = \frac{m}{S_w h}$ is a function reconstructing the fluid density.

Finally, the structure of the single tract PHS is:

$$\left[\begin{array}{c} \dot{\nu_l} \\ \dot{\nu_r} \\ \dot{\pi_y} \\ \dot{m} \\ \dot{h} \\ \hline w_{g0} \equiv \dot{m} \\ w_{g1} \equiv \dot{h} \\ \hline 0 \\ \hline \Psi_l \\ q_r \\ v_w \end{array}\right] = S^{tract} \left[\begin{array}{c} \nabla_{\nu_l} H(x) \equiv q_l \\ \nabla_{\nu_r} H(x) \equiv q_r \\ \nabla_{\pi_y} H(x) \equiv v_w \\ \nabla_m H(x) \equiv \langle \Psi \rangle_\Omega \\ \nabla_h H(x) \equiv -\langle p \rangle_\Omega S w \\ \hline z_{g0}(w_{g1}, \pi_y, m) := v_w \frac{\pi_y}{m} \\ z_{g1}(w_{g0}, \pi_y, m) := -\frac{\pi_y}{m}\dot{m} \\ \hline \lambda_0 \equiv \Psi_l \\ \hline -q_l \\ \Psi_r \\ F_w \end{array}\right], \tag{17}$$

where $< . >_\Omega$ is the volume-average operator. Note that instantaneous laws $z_{g0}(w_{g1}, \pi_y, m)$ and $z_{g1}(w_{g0}, \pi_y, m)$ form a conservative gyrator. The constitutive block matrices of S^{tract} are:

$$S_{xx}^{tract} = \begin{bmatrix} 0 & 0 & 0 & -1 & 0 \\ 0 & 0 & 0 & 1 & 0 \\ 0 & 0 & 0 & 0 & -1 \\ 1 & -1 & 0 & 0 & 0 \\ 0 & 0 & 1 & 0 & 0 \end{bmatrix}, \tag{18a}$$

$$S_{xw}^{tract} = \begin{bmatrix} -1 & 0 \\ 1 & 0 \\ 0 & -1 \\ 0 & 0 \\ 0 & 0 \end{bmatrix}, \tag{18b}$$

$$S_{x\lambda}^{tract} = \begin{bmatrix} -1 \\ 0 \\ 0 \\ 0 \\ 0 \end{bmatrix}, \tag{18c}$$

$$S_{\lambda u}^{tract} = \begin{bmatrix} 1 & 0 & 0 \end{bmatrix}, \tag{18d}$$

$$S_{xu}^{tract} = \begin{bmatrix} 0 & 0 & 0 \\ 0 & -1 & 0 \\ 0 & 0 & 1 \\ 0 & 0 & 0 \\ 0 & 0 & 0 \end{bmatrix}. \tag{18e}$$

This PHS is then a dissipation free model of the tract, controlled by left mass flow q_l, right enthalpy Ψ_r and by the force F_w applied on the wall. Conjugated outputs are the left enthalpy Ψ_l, right mass flow q_r and the speed of the wall v_w. In order to have a mass flow control at the left, a Lagrange multiplier imposing the constraint $-\nabla_{\nu_l} H(x) = -q_l$ has been introduced in (17).

2.3.2 *Assembly of the vocal tract*

Thanks to this Lagrange multiplier, we can now directly connect 2 tracts by linking the outgoing mass flow of the leftmost tract (output of the PHS) to the ingoing mass flow of the rightmost tract (input of the PHS). Repeating this procedure allows to build a full vocal tract composed of an arbitrary number of tracts. Then, we connect simple spring-damper systems to the force inputs for the walls. This aims to represent the effect of the tissues on the dynamics and also provides a control of the walls through their velocity, which is more natural than the force. Finally, a simple radiation condition is added at the rightmost tract. Those last points are explained in more details in [8, chap. 4].

At the end of the assembly, the full vocal tract is controlled by the ingoing input mass flow in the leftmost tract and by velocities of the walls of each tracts.

2.4 Assembly of the full vocal apparatus

From the larynx model and the vocal tract model, the assembly is straightforward: as the output of the larynx is the outgoing volume flow Q^+ and the input of the vocal tract is the mass flow q_l, the connection is achieved by $Q^+/\rho = q_l$, where ρ is the constant density assumed for the glottal flow.

3. NUMERICAL METHOD

The numerical method is based on an adaptation of [12, Chap. 5] to solve a PHS that includes algebraic constraints formulated as in (3). This adaptation corresponds to a projection method that:

- produces solutions in the continuous time-domain (with continuous state and discontinuous effort and flows),
- preserves the power balance, accurate at order 2,
- is capable to manage constraints.

From the original PHS structure given in (3), we define a projected structure

$$\mathcal{S}_P = \{(f,e) \in \mathcal{F}, \mathcal{E} | f = PSe\}, \tag{19}$$

where $P : \mathcal{F} \longmapsto \mathcal{F}$ is a projector over a time interval $\mathbb{T}$. Under the condition that S is skew-symmetric, the projected structure preserves the passivity, that is: $\forall (f,e) \in \mathcal{S}_P, \langle e|f \rangle = 0$. The demonstration is done in [12] for PHS without constraint but the introduction of constraints on efforts does not modify it (as their corresponding flows are always 0). By means of writing the solutions using the basis coefficients in some approximation space, a numerical scheme involving numerical integration at each time step can be developed as in [12]. For our application, we use the simplest case where the approximation space reduces to constants over $\mathbb{T}$, with projector P projecting to this space.

On a given time interval $\mathbb{T}$, variables are then approximated by:

$$x(\tau) := x_0 + h\delta X\tau \Longrightarrow \dot{X}(\tau) = h\delta X, \tag{20a}$$

$$w(\tau) := w_{app}, \tag{20b}$$

$$y(\tau) := y_{app}, \tag{20c}$$

where x_0 is the initial condition (state at $\tau = 0$) and the subscript app stands for approximation. At each time step, we solve the projected PHS for the unknowns δX, w_{app} and y_{app} using the Newton-Raphson method.

4. NUMERICAL EXPERIMENTS

For all our numerical experiments, we use a sampling frequency of 44100 Hz and an absolute tolerance of $1e-10$ for the nonlinear systems solutions.

Configuration	C1	C2	C3
Input pressure amplitude P_0 [Pa]	200	40	200
Vocal folds masses m_i [kg]	$m_r = m_l = 2e-4$	$m_r = m_l = 2e-4$	$m_r = 2e-4$, $m_l = 2.4e-4$
observed regime	damped oscillation	periodic	aperiodic and damped oscillation

Table 1. Parameter sets corresponding to 3 configurations.

4.1 Configurations and regimes

In the following, the assembled model is excited by an input pressure ramp defined by its amplitude P_0, a delay time t_{del} and a rise time t_{rise} such that:

$$P(t) = \begin{cases} 0 & \text{if } t < t_{del}, \\ \frac{t-t_{del}}{t_{rise}} P_0 & \text{if } t_{del} < t < t_{del} + t_{rise}, \\ P_0 & \text{if } t > t_{del} + t_{rise}. \end{cases} \quad (21)$$

For our experiments, we consider a set of fixed parameters for each sub-systems:

- Vocal folds: folds stiffness $k_i = 100$ N.m^{-1}, cover stiffness $\kappa_i = 300$ N.m^{-1}, damping $r_i = 1.3e-3$ kg.s^{-1}, sub-glottal surface $S_{sub} = 11e-5$ m^2 and supra-glottal surface $S_{sup} = 11e-7$ m^2.
- Glottal flow: density $\rho_0 = 1.3$ kg.m^3, length $2l_0 = 4e-3$ m, width $L_0 = 11e-3$ m, initial and reference height $h_0 = h_r = 1e-4$ m.
- Vocal tract: number of tracts $N = 4$, single tract length $2l_0 = 17e-2/(2*N)$ m, tract width $L_0 = 1e-2$ m, initial tract opening $h_{tract} = 1e-2$ m, tracts opening speed $\dot{h}_{tract} = 0$ m.s^{-1}, wall stiffness $k_w = 845$ N.m-3 and wall damping $r_w = 0.04$ kg.s^{-1}.m^2.
- Excitation: delay time $t_{del} = 0.005$ s and rise time $t_{rise} = 0.02$ s.

Table 4 gives 3 sets of the complementary parameters giving rise to 3 different behaviours of the dynamical system. The glottal opening h is shown in figure 4 for the 3 configurations.

In configuration C1, the vocal folds are symmetric and the input pressure amplitude is sufficient to induce self-oscillations of the larynx. After a transient of approximately 0.2 s, the system follows a stable trajectory in which the vocal folds are not touching.

Configuration C2 corresponds to a case where the folds are still symmetrical but the input pressure is low. After a transient, the system converges to a static equilibrium with no oscillations.

In configuration C3, the input pressure amplitude is the same than in configuration C2, but the vocal folds are rendered asymmetrical by changing the mass of the left fold. In that case, the system does not self oscillate but converges slowly to a static regime.

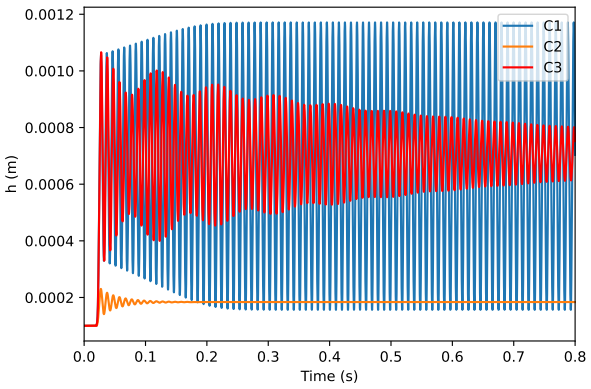

Figure 4. Glottal opening h as a function of time for 3 configurations.

4.2 Cartographies

In order to characterize the parameter sets giving rise to oscillations, we use a cartography methodology based on the work done in [13] for a clarinet model. It is based on the training of a classification algorithm (based on Support Vector Machines) on data gathered from a number of simulations. In this work, we propose a simple two-dimensional cartography of the presented vocal apparatus on the initial glottis opening h_r and on the input pressure amplitude P_0.

The damping coefficient of the vocal folds is set to $4e{-}3$ kg.s^{-1} while the other fixed parameters are the same than presented in part 4.1. Varying parameters h_r [m] and P_0[Pa] are generated using latin hypercube sampling on the intervals $1e-4 < h_r < 1e-3$ and $0 < P_0 < 400$. After running the simulation, we use a criterion based on the envelope of the oscillating signal h (glottis opening) to determine if there is a self-oscillation. If the amplitude of the oscillation is greater at the end of the simulation than just after the transient, we consider that the system is oscillating. Otherwise, we fit the envelope of the oscillation with an equation of type $h(t) = ae^{bt} + c$ and compare the value of c to a criterion value c_{crit}: if $c > c_{crit}$, then we consider that there is an oscillation.

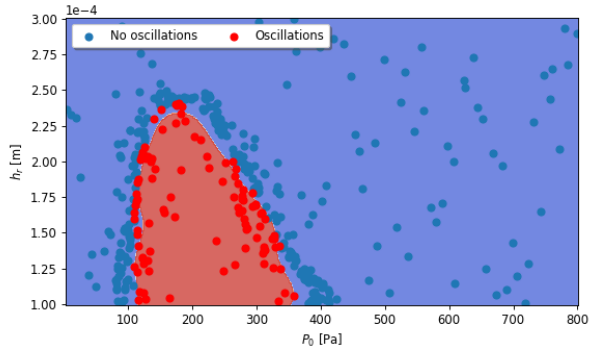

Figure 5. Cartography of oscillating configurations w.r.t. the subglottal pressure P_0 and the glottal opening h_r.

Figure 5 presents the cartography obtained from a number of simulations. We observe that, for the model with chosen fixed parameters, oscillations only occur in a given input pressure range and for a glottal opening at rest below a given value. This is coherent with the fact that abduction of the vocal folds is needed for the apparition of oscillations. Nevertheless, it is important to keep in mind that the lumped parameters values (macroscopic constants) are not straightforward to estimate from the known characteristics of the tissues and that they can greatly influence the shape of the cartography presented figure 5.

5. CONCLUSION AND PERSPECTIVES

The main contribution of this paper is the derivation of a power-balanced simulation of a full vocal apparatus based on a nonlinear lumped-parameter modelling. The model involves fluid-structure interaction with physically interpretable power exchanges. It proves capable to produce self-oscillating regimes, and relevant to characterize such regimes with respect to the sub-glottal pressure and the glottal opening at rest.

A straightforward perspective is to use this model to produce co-articulated sound. In the medium term, further work will concern some modelling of contacts between the vocal folds and a refined description of the exterior domain (fluid loss and acoustic radiation). Another work will be devoted to study methods in order to reduce the computational cost.

6. ACKNOWLEDGMENTS

The authors thank the French National Research Agency for supporting this research work within the AVATARS project (ANR-22-CE48-0014).

7. REFERENCES

[1] K. Ishizaka and J. L. Flanagan, "Synthesis of Voiced Sounds From a Two-Mass Model of the Vocal Cords," *Bell System Technical Journal*, vol. 51, pp. 1233–1268, July 1972.

[2] I. R. Titze, "The human vocal cords: A mathematical model," *Phonetica*, vol. 28, no. 3-4, pp. 129–170, 1973.

[3] B. H. Story and I. R. Titze, "Voice simulation with a body-cover model of the vocal folds," *The Journal of the Acoustical Society of America*, vol. 97, pp. 1249–1260, Feb. 1995.

[4] I. R. Titze and B. H. Story, "Rules for controlling low-dimensional vocal fold models with muscle activation," *The Journal of the Acoustical Society of America*, vol. 112, pp. 1064–1076, Sept. 2002.

[5] X. Zheng, S. Bielamowicz, H. Luo, and R. Mittal, "A Computational Study of the Effect of False Vocal Folds on Glottal Flow and Vocal Fold Vibration During Phonation," *Annals of Biomedical Engineering*, vol. 37, pp. 625–642, Mar. 2009.

[6] X. Zheng, Q. Xue, R. Mittal, and S. Beilamowicz, "A Coupled Sharp-Interface Immersed Boundary-Finite-Element Method for Flow-Structure Interaction With Application to Human Phonation," *Journal of Biomechanical Engineering*, vol. 132, p. 111003, Nov. 2010.

[7] T. Hélie and F. Silva, "Self-oscillations of a vocal apparatus: a port-Hamiltonian formulation," in *Geometric Science of Information: Third International Conference, GSI 2017, Paris, France, November 7-9, 2017, Proceedings* (F. Nielsen and F. Barbaresco, eds.), 3rd conference on Geometric Science of Information (GSI), pp. 375–383, Springer International Publishing, 2017.

[8] V. Wetzel, *Lumped Power-balanced Modelling and Simulation of the Vocal apparatus : a Fluid-Strucutre Interaction Approach*. phdthesis, Sorbonne Université, Dec. 2021.

[9] L. A. Mora, J. I. Yuz, H. Ramirez, and Y. L. Gorrec, "A port-Hamiltonian Fluid-Structure Interaction Model for the Vocal folds," *IFAC-PapersOnLine*, vol. 51, no. 3, pp. 62–67, 2018.

[10] B. Maschke and A. van der Schaft, "Port-Controlled Hamiltonian Systems: Modelling Origins and Systemtheoretic Properties," *IFAC Proceedings Volumes*, vol. 25, pp. 359–365, June 1992.

[11] N. Lopes and T. Hélie, "Energy Balanced Model of a Jet Interacting With a Brass Player's Lip," *Acta Acustica united with Acustica*, vol. 102, pp. 141–154, Jan. 2016.

[12] M. Remy, *Time-continuous power-balanced simulation of nonlinear audio circuits : realtime processing framework and aliasing rejection*. Theses, Sorbonne Université, July 2021.

[13] S. Missoum, C. Vergez, and J.-B. Doc, "Explicit mapping of acoustic regimes for wind instruments," *Journal of Sound and Vibration*, vol. 333, pp. 5018–5029, Sept. 2014.